geoconvention
Virtual Event
September 21-23
2020
CSPG • CSEG • CWLS • GAC • MAC • IAH

Seismicity associated with hydraulic fracturing operations: The influence of complex and competing stress regimes

Rebecca O. Salvage and David W. Eaton
Department of Geosciences, University of Calgary

Summary

On 30 November 2018, three felt (>ML 3.4) earthquakes occurred within the Septimus region of the Montney, which have been attributed to hydraulic fracturing operations. Over 500 events were detected over a 2-week period surrounding the mainshock. All of the events were tightly clustered, both spatially and in depth, and appear to be related to a southern boundary fault of the Fort St. John Graben (FSJG). Stress inversion of a number of focal mechanisms suggests that the maximum principal stress is well constrained and almost horizontal, however the intermediate- and minimum- principal stresses are poorly constrained between the vertical and minimum horizontal stress. This results in a variety of focal mechanisms from the detected seismicity and suggests a high complexity in the local stress regime, explained by the influence of both the Rocky Mountain fold and thrust belt in the north-west, and the FSJG in the south-east.

Theory / Method / Workflow

Seismicity was detected using a local network of 18 three-component seismometers from 27 November to 12 December 2018 using a simple amplitude ratio algorithm (REDPy, Hotovec-Ellis and Jeffries, 2016), followed by a template matching technique to further enhance the catalogue (EQcorrscan, Chamberlain et al., 2017). Using this combined methodology, we identified a total of 594 events from the continuous seismic record over the 15 days of analysis.

Careful manual phase picking was undertaken of 64 template events (those that were identified by an amplitude ratio threshold and therefore had high signal-to-noise). All other events were phase picked automatically using a cross correlation methodology, in which the pick on the new event is defined as the point of maximum correlation with the pick in the template event. Hypocenter locations were then determined using NonLinLoc (Lomax et al., 2000, 2009). Two 1-D velocity models were tested: 1) A 6 layer model used by NRCan to locate seismicity on a regional scale, and 2) a 20 layer model generated from well-log derived P and S wave velocities for the upper 5 km of the crust, smoothed using a median running filter. The well was located approximately 15 km away from the mainshock event. More refined re-locations were gained using HypoDD, which relocates hypocenters based on a double difference algorithm (Waldhauser and Ellsworth, 2000).

Nanometrics performed Moment Tensor Inversions of ten events (including the mainshock and felt aftershocks). Stress inversion of the ten events was carried out using the STRESSINVERSE algorithm (Vavrycuk, 2014) by Suzie Q. Jia (University of Calgary). Using the calculated stresses as input, as well as values from literature, the Fault Slip Potential (FSP) of the southern boundary fault of the FSJG was calculated using the FSP code from Stanford University. FSP is

a method to quantify the probability of inducing slip on a known fault in response to pore fluid pressure changes, based on a Mohr-Coulomb slip criterion.

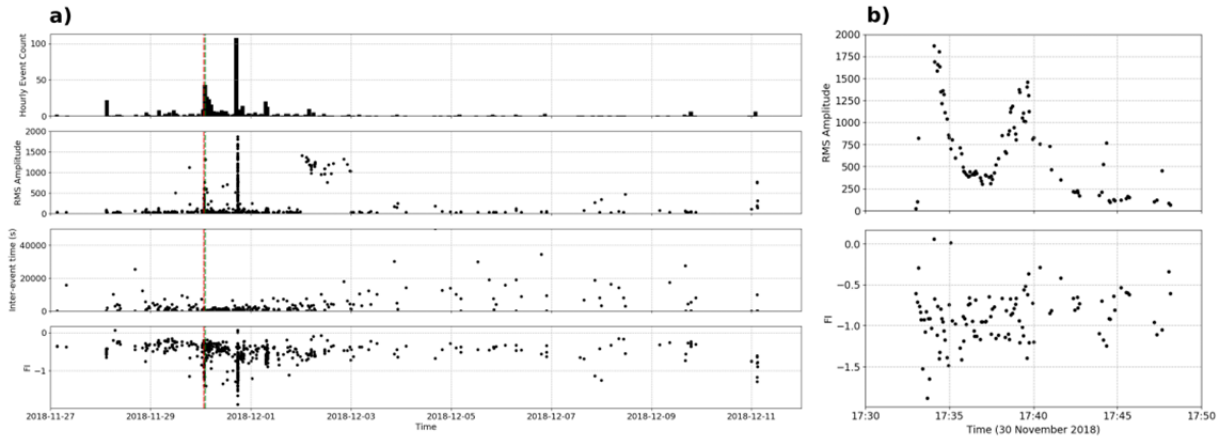

Fig. 1: a) Temporal evolution of seismicity identified from the continuous data using amplitude ratios and template matching. The red vertical line is the timing of the mainshock; green vertical lines are the felt aftershocks. The mainshock and 2 felt aftershock values have been removed from the RMS amplitude panel. b) Amplitude and frequency content of events occurring in a window of ~30 minutes, ~16 hours after the mainshock (largest peak in a).

Results, Observations, Conclusions

The mainshock was shallow (upper 5 km of the crust) and occurred very close to the southern boundary fault of the FSJG. Aftershocks occurred within a tight spatial cluster around the mainshock, with similar depths. Approximately 16 hours after the mainshock, a sudden increase in the number of events was observed over a ~30 minute period. These events had significantly higher RMS amplitudes than the rest of those in the aftershock sequence and contained larger proportions of low frequency energy (Fig. 1a). Furthermore, a complex decay pattern in the aftershock events (amplitudes) was observed following this heightened activity (Fig. 1b).

Hypocenters are tightly clustered around the southern boundary fault of the FSJG and are also tightly clustered in depth (potentially into a semi-planar structure), independent of the velocity model chosen in the upper 5 km of the crust. Fault plane solutions indicate a variety of source mechanisms, including strike-slip, oblique-slip and thrust faulting (Figure 2). The mainshock is represented by oblique reverse faulting (potentially thrust faulting, dependent upon the slip/nodal plane). The two main aftershocks show similar mechanisms, both suggestive of reverse slip motion, however the amount of oblique slip in all three cases varies significantly. In particular towards the west, we see a number of events dominated by thrust-type mechanisms, with more strike-slip and oblique reverse faulting occurring in the east. Our results are in agreement with Amini and Eberhardt (2019), who have suggested that induced seismicity within the Montney play is dominated by a thrust faulting stress regime. They also suggest that this regime is more likely to produce higher magnitude events (such as the ML 4.5 event) than purely strike-slip regimes.

The maximum principal stress direction (sigma 1) is well-constrained and almost horizontal in a NNE-SSW direction. The SHmax direction was calculated as 32.7º. This is slightly rotated from, but still in fair agreement with, the World Stress Map in this area (Heidbach et al., 2016), where borehole breakouts suggest that SHmax direction is in the NE-SW direction at ~45º. The minimum principal stress direction (sigma 3) is also very close to horizontal and the intermediate principal stress direction (sigma 2) is almost vertical, suggesting a dominantly strike-slip regime. However, sigma 2 and sigma 3 are poorly constrained, with synonymous confidence values. This suggests that small changes in stress can result in the reversal of sigma 2 and sigma 3, leading to the diversity in the slip mechanisms observed.

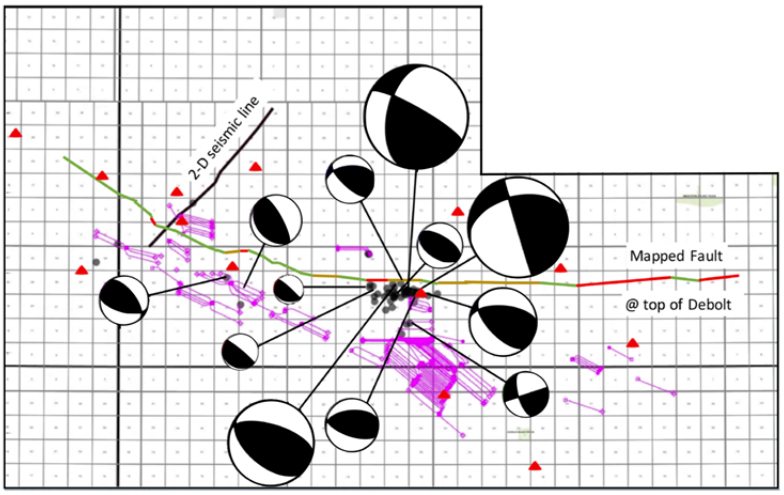

Fig. 2: Focal mechanisms for 10 earthquakes provided by Nanometrics, scaled relative to magnitude. Seismicity = black dots; sensors = red triangles; wells with DFIT data = pink; Southern boundary fault is coloured according to FSP (red = high potential, green = low potential).

The FSP of the southern boundary fault of the FSJG in this study area was carried out by Jieyu Zhang (University of Alberta), and the results are shown in Figure 2. Fault segments that are red have the greatest potential for slip; those coloured green have the least potential. We note that the fault segment most likely associated with the generated seismicity has a relatively high potential for slip (coloured yellow-red). These results suggest that distinct parts of the southern boundary fault of the FSJG may be critically stressed under current conditions.

Novel/Additive Information

The structural complexity introduced by the FSJG is likely to play a significant role in influencing the seismicity in the Fort St. John area. Although the FSJG was formed during a long period of extension during the Carboniferous to Permian (Barclay et al., 1990), the boundary faults show alternating zones of compressional and extensional structures, attributed to the development of the Rocky Mountain fold and thrust belt. This leads to predominantly thrust faulting to the west, and normal faulting in the east (Berger, 1994). Furthermore, the FSJG in the Montney separates the stress regime into dominantly thrust faulting in the north, and strike-slip faulting in the south (Amini and Eberhardt, 2019). Further re-activation of the boundary faults in this area, as seen in

this study, may be due to hydrocarbon recovery (Horner et al., 1994). Since we see evidence of both thrust faulting and strike-slip faulting regimes in the focal mechanisms, it is likely that the cluster of hypocenter locations here sit at the complex confluence of these two large-scale regimes. The confluence of this is responsible for the variety in focal mechanisms, and the fact that very small changes in stress can significantly influence the stress regime between one dominated by strike-slip movement (when sigma 2 is vertical), and one dominated by reverse faulting (when sigma 3 is vertical) (Anderson, 1951).

Acknowledgements

This work was supported by Chevron and the Natural Sciences and Engineering Research Council of Canada (NSERC) through the NSERC/Chevron Industrial Research Chair in Microseismic System Dynamics to DWE. Continuous seismic data were generously provided by ESG Solutions and CNRL. All sponsors of the Microseismic Industry Consortium are also sincerely thanked for their ongoing support and financial contributions. Data processing and analysis was conducted using Obspy (Beyreuther et al., 2010) and the programs mentioned in the text, all of which are open source. We would particularly like to thank Alicia Hotovec-Ellis (USGS) for her unrelenting help in all REDPy matters; Calum Chamberlain (Victoria University, Wellington) for his help regarding EQcorrscan; Jieyu Zhang (University of Alberta) and Suzie Q. Jia (University of Calgary) for carrying out the FSP and stress inversion calculations respectively; and Ron Jackson, Neil Orr, Andy Gamp and Laura Osorio at CNRL for insightful conversations and feedback.

References

Amini, A. and E. Eberhardt (2019). “Influence of tectonic stress regime on the magnitude distribution of induced seismicity events related to hydraulic fracturing”. In: Journal of Petroleum Science and Engineering 182, p. 106284.

Anderson, E. M. (1951). The dynamics of faulting and dyke formation with applications to Britain. Hafner Pub. Co.

Barclay, J. E., F. F. Krause, R. I. Campbell, and J. Utting (1990). “Dynamic casting and growth faulting: Dawson Creek graben complex, Carboniferous-Permian Peace River embayment, western Canada”. In: Bulletin of Canadian Petroleum Geology 38.1, pp. 115–145.
Berger, Z. (1994). Satellite Hydrocarbon Exploration. Springer, Berlin, Heidelberg.

Beyreuther, M., R. Barsch, L. Krischer, T. Megies, Y. Behr, and J. Wassermann (2010). “ObsPy: A Python toolbox for seismology”. In: Seismological Research Letters 81.3, pp. 530–533.

Chamberlain, C. J., C. J. Hopp, C. M. Boese, E. Warren-Smith, D. Chambers, S. X. Chu, K. Michailos, and J. Townend (2017). “EQcorrscan: Repeating and near repeating earthquake detection and analysis in Python”. In: Seismological Research Letters 89.1, pp. 173–181.

Heidbach, O., M. Rajabi, K. Reiter, M. Ziegler, WSM team, et al. (2016). “World stress map database release 2016”. In: GFZ Data Services 10.

Horner, R. B., J. E. Barclay, and J. M. MacRae (1994). “Earthquakes and hydrocarbon production in the Fort St. John area of northeastern British Columbia”. In: Can. J. Explor. Geophys. 30.1, pp. 39–50.

Hotovec-Ellis, A. J. and C. Jeffries (2016). “Near Realtime Detection, Clustering, and Analysis of Repeating Earthquakes: Application to Mount St. Helens and Redoubt Volcanoes - Invited”. In: Seismological Society of America Annual Meeting, Reno, Nevada, 20 April.

Lomax, A., A. Michelini, and A. Curtis (2009). “Earthquake location, direct, global-search methods”. In: Encyclopedia of complexity and systems science, pp. 2449–2473.

Lomax, A., J. Virieux, P. Volant, and C. Berge-Thierry (2000). “Probabilistic earthquake location in 3D and layered models”. In: Advances in seismic event location. Springer, pp. 101–134.

Stanford University (2017). Fault Slip Potential (FSP). Online at: https://scits.stanford.edu/fault-slip-potentialfsp. Last Accessed: 22 October 2019.

Vavrycuk, V. (2014). “Iterative joint inversion for stress and fault orientations from focal mechanisms”. In: Geophysical Journal International 199.1, pp. 69–77.

Waldhauser, F. and W. L. Ellsworth (2000). “A doubledifference earthquake location algorithm: Method and application to the northern Hayward fault, California”. In: Bulletin of the Seismological Society of America 90.6, pp. 1353–1368.